Quantum simulation of quantum field theory using continuous variables

Kevin Marshall,[1] Raphael Pooser,[2,3] George Siopsis,[3,*] and Christian Weedbrook[4]
[1]*Department of Physics, University of Toronto, Toronto, Canada M5S 1A7*
[2]*Quantum Information Science Group, Oak Ridge National Laboratory, Oak Ridge, Tennessee 37831, USA*
[3]*Department of Physics and Astronomy, The University of Tennessee, Knoxville, Tennessee 37996-1200, USA*
[4]*CipherQ, 10 Dundas Street E, Toronto, Canada M5B 2G9*
(Received 31 March 2015; published 14 December 2015)

The year 1982 is often credited as the year that theoretical quantum computing was started with a keynote speech by Richard Feynman, who proposed a universal quantum simulator, the idea being that if you had such a machine you could in principle "imitate any quantum system, including the physical world." With that in mind, we present an algorithm for a continuous-variable quantum computing architecture which gives an exponential speedup over the best-known classical methods. Specifically, this relates to efficiently calculating the scattering amplitudes in scalar bosonic quantum field theory, a problem that is believed to be hard using a classical computer. Building on this, we give an experimental implementation based on continuous-variable states that is feasible with today's technology.

DOI: 10.1103/PhysRevA.92.063825 PACS number(s): 03.67.Ac, 03.67.Lx, 03.70.+k, 42.50.Ex

I. INTRODUCTION

Quantum field theory (QFT) [1] unites the discipline of quantum mechanics with special relativity to provide us with our best understanding of the world around us and what it is made of, notwithstanding that it has yet to be reconciled with general relativity. Typically, the best-known algorithms for calculations in field theories are very difficult on classical computers. One method is lattice field theory [2], which discretizes space into a finite set of points. Unfortunately, classical computations on the lattice increase exponentially with the number of sites, making it unfeasible. Quantum algorithms [3] have been proposed to accomplish a variety of fundamental tasks more quickly than any known classical counterpart, most famously Shor's factoring algorithm [4] and Grover's searching algorithm [5]. When Feynman first proposed the notion of quantum computing [6], he had a different idea in mind, namely, the ability of one quantum system to simulate another [7].

In this paper, we keep true to the spirit of Feynman's vision by presenting a method of calculating scattering amplitudes in a scalar bosonic QFT with a quartic self-interaction on a quantum computing substrate that faithfully encodes the field, i.e., a continuous-variable (CV) quantum computer. In fact, we show one can obtain an exponential speedup over the best-known classical algorithms. A discrete version of this algorithm was originally shown in Refs. [8,9] for a quantum computer based on qubits. Further work extended this result to fermionic QFTs [10], as well as using wavelets for multiscale simulations [11]. Quantum simulators open the door to addressing challenging problems in field theories that would otherwise be impossible with classical methods [12] and this paper presents an important step in that direction.

The field of quantum computing [13] using CVs [14,15] has also progressed significantly in the past few years. From its original conception in 1999 [14], progress began to accelerate after a cluster state [16] version was established in 2006 [17,18], leading to something significantly more tangible for experimentalists. This resulted in numerous proof-of-principle demonstrations [19–22], currently culminating in an extremely large 10 000-node cluster [23] created "on the go" along with a 60-node cluster created simultaneously [24]. From a theoretical perspective, much progress has been made [25–34]. However, one area that is significantly underdeveloped is that of algorithms for a CV quantum computer. Thus far there only exists CV versions of quantum searching [36] and the Deutsch-Jozsa algorithm [37–40].

Typically, q and p are the CVs spreading across all real numbers. To encode them in qubits, one needs a whole register of qubits at each point in space. However, with CVs, there is a one-to-one mapping to qumodes (the CV equivalent of a qubit). In fact it is arguable that a CV quantum computer is the natural choice for such a QFT problem given that the fields are continuous variables. Thus, the value of the field at a given point in space can be mapped onto a qumode naturally. If qubits are used instead, the qumode needs to be replaced by a register of M qubits which only allows the field to take on 2^M discrete values. Brennen *et al.* describe both possibilities in Ref. [11], although they do not explain how to implement the quartic phase gate with CVs, which we do here. Furthermore, the quartic vertex in wavelets becomes very complicated. Implementing it would require gates acting on more than two modes (resulting in logarithmic overhead in complexity).

Another benefit to our approach is in the development of the initial state. Here we show how to create the initial CV state as well as suggesting an experimental implementation based on standard linear optics.

Our paper is structured in the following way. In Sec. II, we discretize space for a one-dimensional scalar bosonic QFT while leaving the field and time as continuous parameters. Next, we show how to generate the initial cluster state using only Gaussian operations in Sec. III. In Sec. IV we outline the steps necessary to compute a scattering amplitude including the required measurement. We provide an explicit experimental implementation in Sec. V. Finally, the benefits of our approach over classical methods are discussed in Sec. VI.

*siopsis@tennessee.edu

II. DISCRETIZATION IN ONE DIMENSION

We consider a relativistic scalar field ϕ in one spatial dimension including a quartic self-interaction. We outline the discretization specifically in the one-dimensional case so as not to clutter the notation unnecessarily, but generalization to higher dimensions is straightforward and is discussed in Appendix D. We note that the field ϕ is a function of x and t (time), $\phi(x,t)$. All three parameters are continuous. In our approach, we discretize x, but not ϕ or t. In the case of qubits, one would discretize x and ϕ, but not t. In classical lattice calculations, one discretizes all three, ϕ, x, and t.

In the continuum, the one-dimensional free-scalar QFT is given by the Hamiltonian

$$H_0 = \frac{1}{2}\int_0^L dx\left[\pi^2 + \left(\frac{\partial\phi}{\partial x}\right)^2 + m^2\phi^2\right], \tag{1}$$

where ϕ is the scalar field and π the conjugate momentum field. They obey commutation relations $[\phi(x),\pi(x')] = i\delta(x-x')$, where we choose units in which $\hbar = 1$.

We discretize space by letting $x = na, n = 0,1,\ldots,N-1$, where a is the lattice spacing and $L = Na$ is the finite length of the spatial dimension ($L \gg a$). We choose units in which $a = 1$, for simplicity, and denote $Q_n = \phi(x)$, $P_n = \pi(x)$. The discretized variables obey standard commutator relations, $[Q_n, P_m] = i\delta_{nm}$. The Hamiltonian becomes

$$H_0 = \sum_{n=0}^{N-1}\frac{P_n^2 + m^2Q_n^2}{2} + \frac{1}{2}\sum_{n=0}^{N-1}(Q_n - Q_{n+1})^2, \tag{2}$$

where we employed periodic boundary conditions and defined $Q_N \equiv Q_0$.

We can write this Hamiltonian as

$$H_0 = \tfrac{1}{2}\mathbf{P}^T\mathbf{P} + \tfrac{1}{2}\mathbf{Q}^T\mathbf{V}\mathbf{Q}, \tag{3}$$

where $\mathbf{P} \equiv [P_0, P_1, \ldots, P_{N-1}]^T$ and $\mathbf{Q} \equiv [Q_0, Q_1, \ldots, Q_{N-1}]^T$. The eigenvalues of the matrix $\mathbf{V}$ and the components of the corresponding normalized eigenvectors $\mathbf{e}^n$ are, respectively, $\omega_n^2 = m^2 + 4\sin^2\frac{n\pi}{N}$ and $\mathbf{e}_k^n = \frac{1}{\sqrt{N}}e^{2\pi ikn/N}, k = 0, \ldots, N-1$. Notice that the massless case is special because it contains a zero mode (for $m = 0$, $\omega_0 = 0$), so the matrix $\mathbf{V}$ is not invertible. To avoid the problems that arise, we can shift the mass by a small amount $\sim 1/N$, which vanishes in the continuum limit ($N \to \infty$).

We also wish to add a quartic interaction, $H_{\rm int} = \frac{\lambda}{4!}\int_0^L dx\phi^4 \to \frac{\lambda}{4!}\sum_n Q_n^4$, which necessitates the addition of a mass counter term $H_{\rm c.t.} = \frac{\delta_m}{2}\int_0^L dx\phi^2 \to \frac{\delta_m}{2}\sum_n Q_n^2$ due to renormalization, as explained in Appendix A. We find that, for weak coupling, the physically interesting case is stable for $\lambda > 0$.

To diagonalize the Hamiltonian, we introduce new creation and annihilation operators, $a_k^\dagger$ and a_k, respectively, defined by $a_k = \sqrt{\frac{\omega_k}{2}}(\mathbf{e}^\dagger\mathbf{Q})_k + \frac{i}{\sqrt{2\omega_k}}(\mathbf{e}^\dagger\mathbf{P})_k$, where $\mathbf{e}$ is the matrix of the eigenvectors. Notice that $\mathbf{e}$ is unitary: $\mathbf{e}^\dagger\mathbf{e} = \mathbf{I}$. These operators obey standard commutation relations, $[a_k, a_l^\dagger] = \delta_{kl}$, and the free Hamiltonian reads

$$H_0 = \sum_{k=0}^{N-1}\omega_k\left(a_k^\dagger a_k + \frac{1}{2}\right). \tag{4}$$

In this form, it is straightforward to construct the states in the Hilbert space.

III. INITIAL-STATE PREPARATION

For the initial state, in Refs. [8,11] the excited state was created *after* creating the ground state. This is difficult because it involves manipulating a large number of qubits. In our approach, we create a single photon state in a single mode *before* creating the initial state. This is more accessible, as it involves creating the state $|1\rangle$ for a single mode. It can be done in a variety of ways, via a heralded single photon source, for instance. At the end of the computation, the field modes are all measured and the distribution of single photons across them determines the result.

To begin with, we build the system with N oscillators representing the variables (Q_n, P_n), $n = 0,1,2,\ldots$. It is useful to define creation and annihilation operators, $A_n^\dagger$ and A_n, respectively, by $A_n = (Q_n + iP_n)/\sqrt{2}$. They obey the commutation relations $[A_n, A_m^\dagger] = \delta_{nm}$. The nth oscillator has a Hilbert space constructed by successive application of the creation operator $A_n^\dagger$ on the vacuum $|0\rangle_n$, which is annihilated by A_n. Here $|0\rangle_n$ is shorthand for a product state of vacuum fields,

$$|0\rangle = |0\rangle_0 \otimes |0\rangle_1 \otimes \cdots \otimes |0\rangle_{N-1}, \tag{5}$$

with $A_n|0\rangle = 0$. For a scattering process, we are given an initial state typically consisting of a fixed number of particles, usually two, which undergoes evolution and then a measurement is performed (detection of particles) on the final state. Both initial and final states asymptote to eigenstates of the free Hamiltonian H_0. Thus, quantum computation starts with preparation of an eigenstate of H_0.

First, we consider the ground state of H_0. It is the state $|\Omega\rangle$ annihilated by all a_k; i.e., $a_k|\Omega\rangle = 0$ for $k = 0,1,\ldots,N-1$. It can be constructed from the vacuum state (5) by acting with the Gaussian unitary $U^\dagger$, where $a_n = U^\dagger A_n U$. Noticing the relationship between the operators a_k and A_k we can use the Bloch-Messiah reduction [41] to determine $U = VSW^\dagger$ as a decomposition involving a multiport interferometer (V) followed by single mode squeezing (S) followed by a final multiport interferometer (W). These unitary operators can be realized with $O(N^2)$ quantum gates [42], although computing the form of these gates requires $O(N^3)$ classical arithmetic operations arising from Gaussian elimination.

To implement U we first perform the rotation

$$\begin{aligned} A_0 &\to A_0' = \sum_{k=0}^{N-1} A_k, \\ A_n &\to A_n' = \sum_{k=0}^{N-1}\cos\frac{2\pi nk}{N}A_k, \\ A_{N-n} &\to A_{N-n}' = \sum_{k=0}^{N-1}\sin\frac{2\pi nk}{N}A_k, \end{aligned} \tag{6}$$

where $1 \leqslant n \leqslant N/2$. This rotation can be expressed as rotations each involving only two oscillators at a time and this fact can lend itself well to the CV cluster state framework [15]. In fact, one could reimagine the algorithm in a cluster state formalism, as all of the requisite interference, squeezing, and nondemolition are present in the state preparation stage. Notice that if N is even, $A_{N/2}$ does not have a partner; we obtain $A_{N/2} \to \sum_k (-)^k A_k$. Next, we squeeze each mode as $A'_n \to A''_n = \cosh r_n A'_n + \sinh r_n A'^{\dagger}_n$, where $e^{2r_n} = \omega_n$ for $n \leqslant N/2$, and $e^{-2r_n} = \omega_n$ for $n > N/2$. Finally, we untangle the pairs by rotating them, $A''_k \to a_k$ where $a_0 = A''_0$, $a_n = (A''_n + iA''_{N-n})/\sqrt{2}$, and $a_{N-n} = (iA''_n + A''_{N-n})/\sqrt{2}$. Excited states can be constructed with the same number of gates; e.g., the single-particle state $|k\rangle \equiv a_k^\dagger|\Omega\rangle$ can be constructed by acting upon the vacuum with $A_k^\dagger$. This turns the initial state of the kth mode into a one-photon state, $A_k^\dagger|0\rangle_k$, which can be accomplished in a variety of ways; see Appendix C. For scattering, we need to create wave packets. For a single-particle wave packet characterized by a profile f_k, which is sharply peaked around some $k = k_0$, we need to create the state $\sum_k f_k A_k^\dagger|0\rangle$. This is an entangled state and can be created with standard techniques. Having engineered the entangled state $\sum_k f_k A_k^\dagger|0\rangle_k$, we then apply the Gaussian unitary $U^\dagger$, to obtain the one-particle wave packet

$$\sum_k f_k a_k^\dagger|\Omega\rangle = U^\dagger \sum_k f_k A_k^\dagger|0\rangle. \tag{7}$$

Extending the above to the engineering of multiparticle states, which are wave packets constructed from the free Hamiltonian eigenstates $|k_1,k_2,\dots\rangle \propto a_{k_1}{}^\dagger a_{k_2}{}^\dagger \cdots |0\rangle$, is a straightforward extension of the procedure outlined above.

IV. QUANTUM COMPUTATION

We wish to calculate a general scattering amplitude, which can be written as

$$\mathcal{A} = \langle \text{out}|T \exp\left\{ i \int_{-T}^{T} dt [H_{\text{int}}(t) + H_{\text{c.t.}}(t)] \right\} |\text{in}\rangle \tag{8}$$

in the limit $T \to \infty$, where time evolution is defined with respect to the noninteracting Hamiltonian.

We start by preparing the initial state $|\text{in}\rangle$ as in the previous section and define initial time as $t = -T$. Then we act successively with evolution operators of the form

$$U(t) = \exp\{i\delta t[H_{\text{int}}(t) + H_{\text{c.t.}}(t)]\}. \tag{9}$$

Time dependence is obtained via the free Hamiltonian,

$$Q_i(t) = e^{itH_0} Q_i(0) e^{-itH_0}. \tag{10}$$

Therefore, the evolution (9) can be implemented as

$$U(t) = e^{itH_0} e^{i\delta t(H_{\text{int}}+H_{\text{c.t.}})} e^{-itH_0}. \tag{11}$$

We deduce

$$\mathcal{A} = \langle \text{out}|[e^{i\delta t H_0} e^{i\delta t(H_{\text{int}}+H_{\text{c.t.}})}]^N |\text{in}\rangle, \tag{12}$$

where we divided the time interval into $N = \frac{2T}{\delta t}$ segments.

The coupling constants in Eq. (9) are turned on and off adiabatically. This is achieved by splitting the time interval $[-T,T]$ into three segments, $[-T,-T_1]$, $[-T_1,T_1]$, and $[T_1,T]$. For $t \in [-T,-T_1]$, we turn the coupling constants on by replacing $\lambda \to \lambda(t)$, $\delta m \to \delta m(t)$, so that $\lambda(-T) = \delta m(-T) = 0$, and $\lambda(-T_1) = \lambda$, $\delta m(-T_1) = \delta m$. Then for $t \in [-T_1,T_1]$ the coupling constants are held fixed. Finally, for $t \in [T_1,T]$, they are turned off adiabatically by reversing the process in the first time interval. In the case of small λ, the time dependence of the coupling constants can be chosen efficiently by making use of perturbative renormalization. Renormalization informs the choice (see Appendix A) $\lambda(t) = \frac{T+t}{T-T_1}\lambda$, $\delta m(t) = \frac{\lambda(t)}{8\pi} \log \frac{64}{m^2}$, for $-T \leqslant t \leqslant -T_1$.

The unitary operators $e^{i\delta t H_0}$ and $e^{i\delta t H_{\text{c.t.}}}$ are Gaussian and can be implemented with second-order nonlinear optical interactions and linear optics beam-splitter networks. The interaction is implemented through a *quartic* phase gate for each mode,

$$e^{i\delta t H_{\text{int}}} = \prod_n e^{i\gamma Q_n^4}, \quad \gamma = \delta t \frac{\lambda}{4!}. \tag{13}$$

The quartic phase gate may be implemented in a similar manner to the cubic phase gate previously proposed [25].

After evolution, we must measure the system in a basis containing the projection corresponding to the state $|\text{out}\rangle$. This is similar to the state $|\text{in}\rangle$, and its construction depends on the number of desired particles. The latter are excitations created with $a_n^\dagger$, so in general,

$$|\text{out}\rangle = a_{n_1}^\dagger a_{n_2}^\dagger \cdots |\Omega\rangle = U^\dagger A_{n_1}^\dagger A_{n_2}^\dagger \cdots |0\rangle. \tag{14}$$

It follows that the next step is to *uncompute* by applying the Gaussian unitary U (which is the inverse operation to the preparation of the initial state) and then measure the number of photons in each mode. The final uncompute step projects the set of output modes onto the Fock basis which we then sample from. Thus, the scattering amplitude calculation is a mapping from one set of field modes on the input to a separate set of field modes on the output, as expected. That is, for each click on the photodetector for mode n, there is an operator $a_n^\dagger$ present in the final state (14). If the QFT calculation involved an initial input state with two excitations spread across 100 field modes, say, then the entire calculation would involve two photons, for instance. We note that the calculation has made use of a quartic phase gate up to this point, and thus technically speaking a non-Gaussian operation would not be necessary during this measurement step in order to achieve an exponential speedup over the classical QFT algorithm. However, in order to achieve high accuracy in the final result, photon-number-resolving detectors with high efficiency [43] would be desirable for the measurement phase.

V. EXPERIMENTAL IMPLEMENTATION

An example of the experimental implementation is given in Fig. 1. For brevity the setup for calculating four space-time points is given. For the electromagnetic field, the initial unitary rotation involves weighted beam splitters with the appropriate splitting to achieve the desired sums over the field operators (see Appendix B). A swap gate is involved in the input state preparation stage. We note that a swap gate contains essentially the CV version of the controlled-NOT operator along with parity operators [44], but in some cases the gate

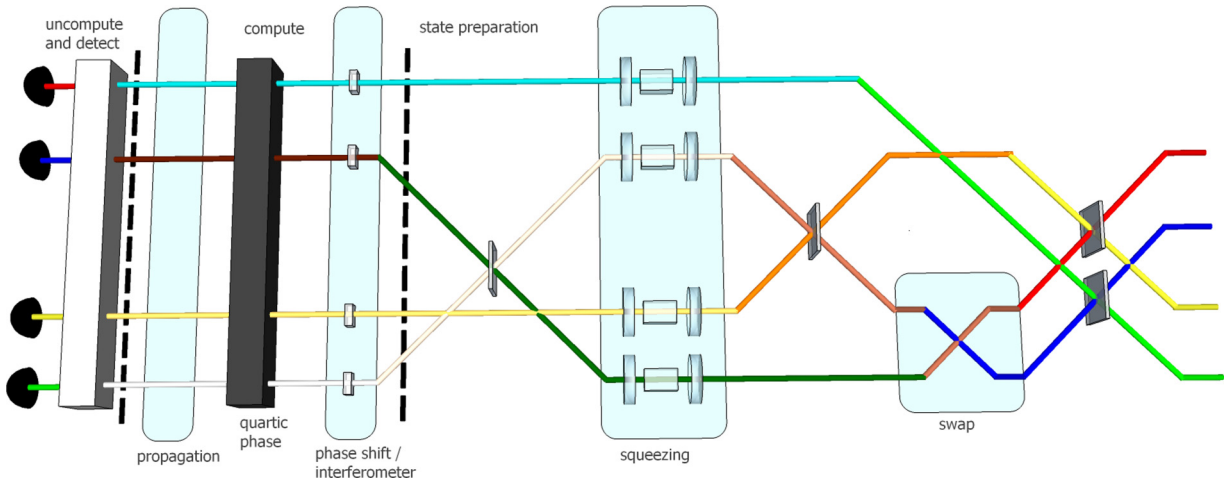

FIG. 1. (Color online) Sketch of an experimental setup for electromagnetic field modes used as qudits in a QFT calculation involving four field modes. The modes are encoded into electric field modes (red, blue, yellow, and green), which are then prepared via beam splitters, swap gates, and squeezers for the compute stage. The compute stage consists of an interferometer, a quartic phase gate (black box; see Ref. [25]), and free propagation. An uncompute stage, which is the inverse of the preparation stage, and a detection stage in the Fock basis yield the scattering amplitudes into the four QFT field modes.

can be simplified to a beam-splitter interaction [45] such as for the electromagnetic field. Here we use a mode label swap operator, which is possible in systems with movable qubits, such as CV optical fields. Next, $H_{\text{c.t.}}$ is quadratic in position quadrature operators, which can be implemented with a series of phase shifts [45]. The non-Gaussian piece of the computation is then the quartic phase gate contained in H_{int}, which can be implemented via repeated application of the photon-number-dependent phase gate [25]. Lastly, the free propagation H_0 can be implemented by a calibrated free propagation before the uncompute stage. We note that the QFT field modes are encoded into the qudits which are themselves electromagnetic field modes, meaning that the free propagation contained in H_0 is not arbitrary. It must conform to the calculated QFT free propagation distance, and phase stability must be maintained throughout.

VI. CONCLUSION

In conclusion, we developed an algorithm for a continuous-variable quantum computer which gave an exponential speedup over the best-known classical algorithms. This algorithm was the calculation of the scattering amplitudes in scalar bosonic quantum field theory, and, as previously mentioned, arguably a natural choice for a continuous-variable quantum computer to solve. At weak coupling, analytic calculations are possible; however, at strong coupling no such calculations are generally available, and one has to rely on numerical techniques. A widely used framework is lattice field theory which is based on the discretization of space into a finite set of points. The complexity of classical computations on a lattice increases exponentially with the number of lattice sites [2].

Quantum computations offer a distinct advantage (first shown in Ref. [9] for qubits, and here for qumodes), since complexity only grows polynomially. Finally, we also gave an example of an experimental implementation on a continuous-variable quantum computer that calculated four space-time points. We noted that such a scheme is feasible with current linear optical technology and consisted of a set of Gaussian operations along with the non-Gaussian quartic phase gate.

ACKNOWLEDGMENTS

We are grateful to Peter Rohde for feedback. K.M. acknowledges support from NSERC. R.C.P. performed portions of this work at Oak Ridge National Laboratory, operated by UT-Battelle for the U.S. Department of Energy under Contract No. DE-AC05-00OR22725.

APPENDIX A: RENORMALIZATION

Define the Green's function $\mathbf{G}(t_1,t_2)$ as

$$G_{ij}(t_1,t_2) = \langle 0|\mathcal{T}(Q_i(t_1)Q_j(t_2))|0\rangle, \tag{A1}$$

where $\mathcal{T}$ denotes the time-ordering operator. It obeys

$$\left[\partial_{t_1}^2 + \mathbf{V}\right]\mathbf{G}(t_1,t_2) = -i\mathbf{I}\delta(t_1 - t_2). \tag{A2}$$

Using the Fourier transform,

$$\mathbf{G}(t_1,t_2) = \int \frac{d\omega}{2\pi} e^{i\omega(t_1-t_2)}\tilde{\mathbf{G}}(\omega), \tag{A3}$$

we obtain

$$\tilde{\mathbf{G}}(\omega) = i[-\omega^2\mathbf{I} + \mathbf{V}]^{-1} = \sum_n \frac{-i}{\omega^2 - \omega_n^2}\mathbf{e}_n\mathbf{e}_n^\dagger, \tag{A4}$$

exhibiting poles at $\omega^2 = \omega_n^2$.

When we switch on the interaction term,

$$H_{\text{int}} = \frac{\lambda}{4!}\int_0^L dx\phi^4 \to \frac{\lambda}{4!}\sum_n Q_n^4, \tag{A5}$$

we have that at $O(\lambda)$ the Green's function is corrected by

$$\delta G_{ij}(t_1,t_2) = \langle 0|\mathcal{T}\left[Q_i(t_1)Q_j(t_2)\int dt H_{\text{int}}(t)\right]|0\rangle. \tag{A6}$$

For the Fourier transform, we obtain

$$\delta\tilde{\mathbf{G}}(\omega) = \lambda[\tilde{\mathbf{G}}(\omega)]^2 \int \frac{d\omega'}{2\pi} \mathrm{Tr}\,\tilde{\mathbf{G}}(\omega'), \tag{A7}$$

which leads to a shift of the poles,

$$\tilde{\mathbf{G}}(\omega) + \delta\tilde{\mathbf{G}}(\omega) = \sum_n \frac{-i}{\omega^2 - \omega_n^2 - \Sigma} \mathbf{e}_n \mathbf{e}_n^\dagger + O(\lambda^2), \tag{A8}$$

where

$$\Sigma = \frac{\lambda}{2N} \int \frac{d\omega'}{2\pi} \sum_n \frac{-i}{\omega'^2 - \omega_i^2} = \frac{\lambda}{4N} \sum_n \frac{1}{\omega_n}. \tag{A9}$$

The shift can be corrected by the addition of the counter term

$$H_{\text{c.t.}} = \frac{\delta_m}{2} \int_0^L dx \phi^2 \to \frac{\delta_m}{2} \sum_n Q_n^2, \tag{A10}$$

with $\delta_m = -\Sigma + O(\lambda^2)$, i.e., the mass parameter in the Hamiltonian is not physical, but bare:

$$m_0^2 = m^2 + \delta_m = m^2 - \frac{\lambda}{4N} \sum_n \frac{1}{\omega_n} + O(\lambda^2). \tag{A11}$$

For large N, the sum can be approximated by an integral,

$$\Sigma = \frac{\lambda}{4} \int_0^1 \frac{dk}{\sqrt{m^2 + 4\sin^2 k\pi}}, \tag{A12}$$

which has a logarithmic divergence at small m^2 (i.e., length scale $1/m$ large in units of lattice spacing, which is the physically interesting limit). We easily obtain

$$\Sigma = \frac{\lambda}{8\pi} \log \frac{64}{m^2} + O(m^2). \tag{A13}$$

The bare mass is

$$m_0^2 = m^2 - \Sigma + O(\lambda^2) = m^2 - \frac{\lambda}{8\pi} \log \frac{64}{m^2} + O(\lambda^2, m^2). \tag{A14}$$

Notice that for weak coupling (small λ), the physically interesting case has $m_0^2 < 0$ (a stable system, as long as $\lambda > 0$).

APPENDIX B: GROUND-STATE CONSTRUCTION

To find the required transformation U, we work as follows. Notice that for $n = 0$,

$$a_0 = \frac{1}{2\sqrt{N}} \sum_{k=0}^{N-1} \left[\left(\sqrt{m} + \frac{1}{\sqrt{m}} \right) A_k + \left(\sqrt{m} - \frac{1}{\sqrt{m}} \right) A_k^\dagger \right], \tag{B1}$$

where we used $\omega_0 = m$. For $n \neq 0$, we consider pairs (a_n, a_{N-n}). We have

$$\begin{aligned} a_n + a_{N-n} &= \frac{1}{2\sqrt{N}} \sum_{k=0}^{N-1} \cos \frac{2\pi nk}{N} \left[\left(\sqrt{\omega_n} + \frac{1}{\sqrt{\omega_n}} \right) A_k + \left(\sqrt{\omega_n} - \frac{1}{\sqrt{\omega_n}} \right) A_k^\dagger \right], \\ a_n - a_{N-n} &= \frac{i}{2\sqrt{N}} \sum_{k=0}^{N-1} \sin \frac{2\pi nk}{N} \left[\left(\sqrt{\omega_n} + \frac{1}{\sqrt{\omega_n}} \right) A_k - \left(\sqrt{\omega_n} - \frac{1}{\sqrt{\omega_n}} \right) A_k^\dagger \right], \end{aligned} \tag{B2}$$

where we used $\omega_n = \omega_{N-n}$.

The above expressions suggest that we transform A_n into a_n in three steps, as shown in the main text.

Example: $N = 4$

To illustrate the above algorithm, we consider the case in which space has been discretized to four points. The rotation ($\mathbf{A}' = \mathbf{OA}$) is described by the orthogonal matrix

$$\mathbf{O} = \frac{1}{2} \begin{bmatrix} 1 & 1 & 1 & 1 \\ \sqrt{2} & 0 & -\sqrt{2} & 0 \\ 1 & -1 & 1 & -1 \\ 0 & \sqrt{2} & 0 & -\sqrt{2} \end{bmatrix}. \tag{B3}$$

We have

$$\mathbf{O} = R_{02}\left(\frac{\pi}{4}\right) S_{01} R_{13}\left(\frac{\pi}{4}\right) R_{02}\left(\frac{\pi}{4}\right), \tag{B4}$$

where $R_{ij}(\theta)$ is a rotation in the ij plane of angle θ and S_{ij} is the swap $i \leftrightarrow j$. Therefore, the rotation $\mathbf{O}$ can be implemented with four two-mode unitaries.

Next, we squeeze each mode as $A_n' \to A_n'' = \cosh r_n A_n' + \sinh r_n A_n'^\dagger$, where $e^{2r_0} = \omega_0$, $e^{2r_1} = \omega_1$, $e^{2r_2} = \omega_2$, and $e^{-2r_3} = \omega_3$. Notice that $r_3 = -r_1$, because $\omega_3 = \omega_1$.

Finally, we perform the rotation, $A_1'' \to \frac{1}{\sqrt{2}}(A_1'' + iA_3'')$, $A_3'' \to \frac{1}{\sqrt{2}}(iA_1'' + A_3'')$, to arrive at the desired modes,

$$\begin{aligned} a_0 &= \frac{1}{2} \sum_n \left[\cosh r_0 A_n + \sinh r_0 \sum_n A_n^\dagger \right], \\ a_1 &= \frac{1}{2} \sum_n i^n \left[\cosh r_1 A_n + \sinh r_1 \sum_n A_n^\dagger \right], \\ a_2 &= \frac{1}{2} \sum_n (-1)^n \left[\cosh r_2 A_n + \sinh r_2 \sum_n A_n^\dagger \right], \\ a_3 &= \frac{1}{2} \sum_n (-i)^n \left[\cosh r_3 A_n + \sinh r_3 \sum_n A_n^\dagger \right]. \end{aligned} \tag{B5}$$

Each of the above steps is implemented with a Gaussian unitary involving at most two modes.

APPENDIX C: EXCITED STATES

To generate the required one-photon state, two methods can be used. One can first squeeze the vacuum of the kth mode with an optical parametric amplifier to

$$S_k(s)|0\rangle_k, \quad S_k(s) = e^{\frac{s}{2}(A_k^{\dagger 2} - A_k^2)}. \tag{C1}$$

Then pass the squeezed state through a (highly transmitting) beam splitter of transmittance T, and place a photodetector on the auxiliary output port. A click of the detector heralds a successful photon subtraction, which is described by the nonunitary operator

$$\sqrt{1-T}\, T^{A_k^\dagger A_k/2} A_k. \tag{C2}$$

The transmittance has to be high so that the probability of detecting two or more photons is negligible. If no photon is detected, the process is repeated until a photon is detected. Finally, apply antisqueezing $S_k^\dagger(s')$.

We obtain the state (unnormalized)

$$S_k^\dagger(s') T^{A_k^\dagger A_k/2} A_k S_k(s)|0\rangle_k. \tag{C3}$$

If the squeezing parameters are chosen so that

$$T = \frac{\tanh s'}{\tanh s}, \tag{C4}$$

then it is straightforward to show that (C3) is the desired state,

$$S_k^\dagger(s') T^{A_k^\dagger A_k/2} A_k S_k(s)|0\rangle_k \propto A_k^\dagger|0\rangle_k. \tag{C5}$$

Optionally, one may also use a heralded single photon source. Such a source would consist of a parametric down-converter with a high-efficiency heralding detector. To obtain exactly one photon when operating the source with high brightness (but on average less than one pair per pulse), the heralding detector would consist of a high-efficiency photon-number-resolving detector, such as a transition edge sensor.

APPENDIX D: GENERALIZATION TO ARBITRARY DIMENSIONS

Generalization to arbitrary spatial dimension d is straightforward. The free-scalar Hamiltonian in the continuum reads

$$H_0 = \frac{1}{2}\int d^d x [\pi^2 + (\nabla\phi)^2 + m^2\phi^2], \tag{D1}$$

where $\mathbf{x} \in [0, L]^d$, with the fields obeying standard commutation relations,

$$[\phi(\mathbf{x}),\, \pi(\mathbf{x}')] = i\delta^d(\mathbf{x} - \mathbf{x}'). \tag{D2}$$

Each coordinate x_i $(i = 1, \ldots, d)$ is discretized as before, $x_i = n_i a$, $n_i = 0, 1, \ldots, N-1$, and we define $Q_\mathbf{n} \equiv \phi(\mathbf{x})$, $P_\mathbf{n} \equiv \pi(\mathbf{x})$, and $A_\mathbf{n} = \frac{1}{\sqrt{2}}(Q_\mathbf{n} + iP_\mathbf{n})$, where $\mathbf{n} \in \mathbb{Z}_N^d$.

The Hamiltonian (D1) can then be rendered in the form

$$H_0 = \tfrac{1}{2}\mathbf{P}^T\mathbf{P} + \tfrac{1}{2}\mathbf{Q}^T\mathbf{V}\mathbf{Q}, \tag{D3}$$

where $\mathbf{V}$ has eigenvalues and corresponding normalized eigenvectors,

$$\begin{aligned} \omega_\mathbf{k}^2 &= m^2 + 4\sum_{i=1}^d \sin^2\frac{k_i}{2}, \\ \mathbf{e}_\mathbf{k}^\mathbf{n} &= \frac{1}{N^{d/2}} e^{i\mathbf{k}\cdot\mathbf{n}}, \end{aligned} \tag{D4}$$

where $\mathbf{k} \in \frac{2\pi}{N}\mathbb{Z}_N^d$ (the dual lattice). The eigenvectors form a unitary matrix.

The discretized Hamiltonian is diagonalized as

$$H_0 = \sum_{\mathbf{k}\in\Gamma} \omega_\mathbf{k}\left(a_\mathbf{k}^\dagger a_\mathbf{k} + \frac{1}{2}\right), \tag{D5}$$

where $a_\mathbf{k}$ is the annihilation operator (extended to d dimensions in an obvious way).

Introducing an interaction term, $H_{\text{int}} = \frac{\lambda}{4!}\sum_\mathbf{n} Q_\mathbf{n}^4$, and the attendant counter term, $H_{\text{c.t.}} = \frac{\delta_m}{2}\sum_\mathbf{n} Q_\mathbf{n}^2$, and working as in the one-dimensional case, we obtain a shift in the poles of the Green's function,

$$\Sigma = \frac{\lambda}{4}\sum_{\mathbf{k}\in\Gamma}\frac{1}{\omega_\mathbf{k}} + O(\lambda^2), \tag{D6}$$

which is related to the counter-term parameter δ_m via $\delta_m = -\Sigma + O(\lambda^2)$. For large N, the sum is approximated by an integral over the hypercube $[0, 2\pi]^d$. For $d = 1$, it reduces to the previous result, whereas for $d > 1$, we obtain at lowest order in m and λ,

$$\Sigma = C_d\lambda + \cdots. \tag{D7}$$

Numerically, $C_2 \approx 0.16$, and $C_3 \approx 0.11$.

[1] M. E. Peskin and D. V. Schroeder, *An Introduction to Quantum Field Theory* (Westview Press, Boulder, CO, 1995).

[2] M. Creutz, *Quarks, Gluons and Lattices* (Cambridge University Press, Cambridge, UK, 1985), Vol. 8.

[3] M. A. Nielsen and I. L. Chuang, *Quantum Computation and Quantum Information* (Cambridge University Press, Cambridge, UK, 2010).

[4] P. Shor, SIAM J. Comput. **26**, 1484 (1997).

[5] L. K. Grover, Phys. Rev. Lett. **79**, 325 (1997).

[6] R. Feynman, Int. J. Theor. Phys. **21**, 467 (1982).

[7] I. M. Georgescu, S. Ashhab, and F. Nori, Rev. Mod. Phys. **86**, 153 (2014).

[8] S. P. Jordan, K. S. M. Lee, and J. Preskill, Science **336**, 1130 (2012).

[9] S. P. Jordan, K. S. M. Lee, and J. Preskill, Quantum Inf. Comput. **14**, 1014 (2014).

[10] S. P. Jordan, K. S. M. Lee, and J. Preskill, arXiv:1404.7115.

[11] G. K. Brennen, P. Rohde, B. C. Sanders, and S. Singh, Phys. Rev. A **92**, 032315 (2015).

[12] U.-J. Wiese, Ann. Phys. **525**, 777 (2013).

[13] T. D. Ladd *et al.*, Nature (London) **464**, 45 (2010).

[14] S. Lloyd and S. L. Braunstein, Phys. Rev. Lett. **82**, 1784 (1999).

[15] C. Weedbrook, S. Pirandola, R. García-Patrón, N. J. Cerf, T. C. Ralph, J. H. Shapiro, and S. Lloyd, Rev. Mod. Phys. **84**, 621 (2012).
[16] R. Raussendorf and H. J. Briegel, Phys. Rev. Lett. **86**, 5188 (2001).
[17] J. Zhang and S. L. Braunstein, Phys. Rev. A **73**, 032318 (2006).
[18] N. C. Menicucci, P. van Loock, M. Gu, C. Weedbrook, T. C. Ralph, and M. A. Nielsen, Phys. Rev. Lett. **97**, 110501 (2006).
[19] S. Yokoyama, R. Ukai, S. C. Armstrong, J.-i. Yoshikawa, P. van Loock, and A. Furusawa, Phys. Rev. A **92**, 032304 (2015).
[20] K. Miyata, H. Ogawa, P. Marek, R. Filip, H. Yonezawa, J.-i. Yoshikawa, and A. Furusawa, Phys. Rev. A **90**, 060302 (2014).
[21] M. Pysher, Y. Miwa, R. Shahrokhshahi, R. Bloomer, and O. Pfister, Phys. Rev. Lett. **107**, 030505 (2011).
[22] S. Takeda, T. Mizuta, M. Fuwa, J.-i. Yoshikawa, H. Yonezawa, and A. Furusawa, Phys. Rev. A **87**, 043803 (2013).
[23] S. Yokoyama, R. Ukai, S. C. Armstrong, C. Sornphiphatphong, T. Kaji, S. Suzuki, J.-i. Yoshikawa, H. Yonezawa, N. C. Menicucci, and A. Furusawa, Nat. Photonics **7**, 982 (2013).
[24] M. Chen, N. C. Menicucci, and O. Pfister, Phys. Rev. Lett. **112**, 120505 (2014).
[25] K. Marshall, R. Pooser, G. Siopsis, and C. Weedbrook, Phys. Rev. A **91**, 032321 (2015).
[26] H.-K. Lau and C. Weedbrook, Phys. Rev. A **88**, 042313 (2013).
[27] P. van Loock, C. Weedbrook, and M. Gu, Phys. Rev. A **76**, 032321 (2007).
[28] M. Gu, C. Weedbrook, N. C. Menicucci, T. Ralph, and P. van Loock, Phys. Rev. A **79**, 062318 (2009).
[29] R. N. Alexander, S. C. Armstrong, R. Ukai, and N. C. Menicucci, Phys. Rev. A **90**, 062324 (2014).
[30] T. F. Demarie, T. Linjordet, N. C. Menicucci, and G. K. Brennen, New J. Phys. **16**, 085011 (2014).
[31] N. C. Menicucci, T. F. Demarie, and G. K. Brennen, arXiv:1503.00717.
[32] P. Wang, M. Chen, N. C. Menicucci, and O. Pfister, Phys. Rev. A **90**, 032325 (2014).
[33] N. C. Menicucci, Phys. Rev. A **83**, 062314 (2011).
[34] N. C. Menicucci, Phys. Rev. Lett. **112**, 120504 (2014).
[35] D. Gottesman, A. Kitaev, and J. Preskill, Phys. Rev. A **64**, 012310 (2001).
[36] A. K. Pati, S. L. Braunstein, and S. Lloyd, arXiv:quant-ph/0002082.
[37] A. K. Pati and S. L. Braunstein, in *Quantum Information with Continuous Variables*, edited by S. L. Braunstein and A. K. Pati (Kluwer Academic, Dordrecht, 2003), pp. 31–36.
[38] M. R. A. Adcock, P. Høyer, and B. C. Sanders, New J. Phys. **11**, 103035 (2009).
[39] M. Zwierz, C. A. Pérez-Delgado, and P. Kok, Phys. Rev. A **82**, 042320 (2010).
[40] M. R. A. Adcock, P. Høyer, and B. C. Sanders, Quantum Inf. Process. **12**, 1759 (2013).
[41] S. L. Braunstein, Phys. Rev. A **71**, 055801 (2005).
[42] M. Reck, A. Zeilinger, H. J. Bernstein, and P. Bertani, Phys. Rev. Lett. **73**, 58 (1994).
[43] A. E. Lita, A. J. Miller, and S. Nam, Opt. Express **16**, 3032 (2008).
[44] X. Wang, J. Phys. A: Math. Gen. **34**, 9577 (2001).
[45] S. L. Braunstein and P. van Loock, Rev. Mod. Phys. **77**, 513 (2005).